

Comprehensive Liver Imaging Using Multi-Parametric MRI and Ultrasound



Richard G. Barr MD, PhD, FACR, FSRU, FAIUM, FSAR
Professor of Radiology
Northeastern Ohio Medical University



Wissam AlGhuraibawi, PhD
Medical Affairs Manager, Clinical Scientist
Canon Medical Systems USA



Todd N. Erpelding, PhD
Ultrasound Medical Affairs Leader
Canon Medical Systems USA

Introduction

Chronic liver disease (CLD) is a major cause of mortality, morbidity, and high healthcare expenditure. In the United States, CLD was responsible for more than 54,000 deaths in 2022 and has a projected economic impact on the healthcare system of \$1 trillion in 2024.^{1,2} The clinical management of patients with CLD has benefited from the emergence of quantitative imaging biomarkers of liver fibrosis, fat, and iron, which are used for diagnosis, staging, disease monitoring, and treatment response assessment.³ The emergence of non-invasive MRI and ultrasound techniques to quantitatively measure and map liver biomarkers has rapidly replaced the traditional biopsy procedures in many patient care settings.

In addition to routine clinical MR imaging for the liver, such as T1, T2, MRCP, and MRA, Canon offers proton density fat fraction (PDFF) and magnetic resonance elastography (MRE) techniques. Canon implemented a multi-echo 3D FE sequence in a single breath-hold to simultaneously generate in-phase (IP), out-of-phase (OP), fat-only, water-only images, and quantitative maps of liver fat as well as transverse relaxation rate ($R2^*$). Clinically $R2^*$ maps are usually used to estimate liver iron deposition.⁴ Similarly, MRE maps can be generated using FE 2D (in 4 breath-holds) or SE-EPI 2D (in a single breath-hold) acquisitions.

Grayscale and Doppler ultrasound are commonly used in liver assessment, as well. Canon offers a quantitative ultrasound liver analysis package including shear wave elastography (SWE), shear

wave dispersion, and attenuation imaging (ATI) which can aid in the diagnosis and monitoring of CLD, including metabolic dysfunction-associated steatotic liver disease (MASLD) and metabolic dysfunction-associated steatohepatitis (MASH).

These case studies demonstrate the capability of multi-parametric MRI and ultrasound techniques to provide comprehensive liver studies at Southwoods Imaging in Boardman, Ohio.

Case 1

History: A 75-year-old male patient was referred to the imaging center for a liver MRI. The patient has a history of alcoholic cirrhosis. In 2018, he was diagnosed with compensated advanced chronic liver disease (cACLD), and in 2021, progressed to decompensated cirrhosis. Currently, the patient is on the liver transplant list.

Imaging Findings: Clinical images were acquired on the Canon Galan 3T MRI and Canon Aplio i800 ultrasound system. Imaging findings demonstrated the decreased size of the right liver lobe with nodular heterogeneous liver surface, abdominal ascites, and no focal liver lesions. Portal vein flow remains hepatopetal.

MR PDFF and ultrasound ATI scans showed normal liver fat (S0) measurements (PDFF average 4.8%, ATI median 0.58 dB/cm/

MHz), as shown in Figure 1.^{5,6} Elevated $R2^*$ (averaged 185.6/sec) was measured, which is usually linked to liver iron overload.⁷

MRE exams have been implemented using both FE 2D and SE-EPI 2D MRE sequences. Due to elevated $R2^*$ measurements, the amplitude images for the FE 2D acquisition demonstrated reduced SNR, which consequently resulted in an unreliable

stiffness map (Fig. 2, upper row). Ultrasound SWE was unreliable (IQR/median [m/s] = 0.36), as well. On the other hand, amplitude, wave, and stiffness map images acquired from the SE-EPI 2D MRE acquisition were reliable and demonstrated elevated liver stiffness measurements consistent with advanced fibrosis (Averaged 4.6 kPa, Fig. 2, lower row).

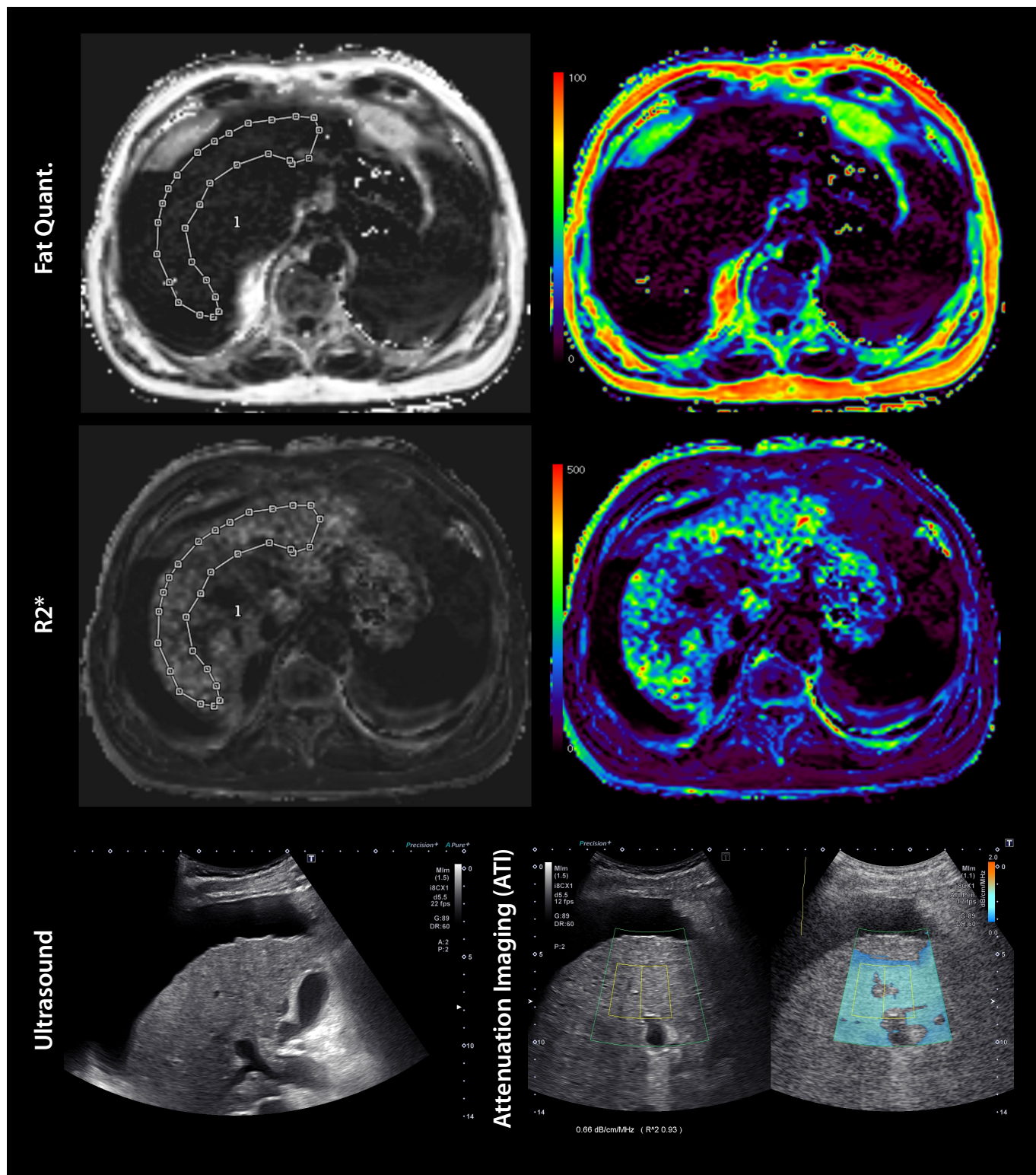


Figure 1: Top row: Fat quantification map from the axial mecho FE 3D PDFF scan with normal fat measurements averaged 4.8% and colored map. Middle row: Generated transverse relaxation rate $R2^*$ and colored maps. The patient demonstrated elevated $R2^*$ measurements (shortened $T2^*$) averaging 185.6/sec. Bottom row: Grayscale ultrasound showing nodular liver surfaces and ascites. Median ATI measurement was 0.58 dB/cm/MHz, which is consistent with PDFF indication of normal liver fat (no steatosis, S0).

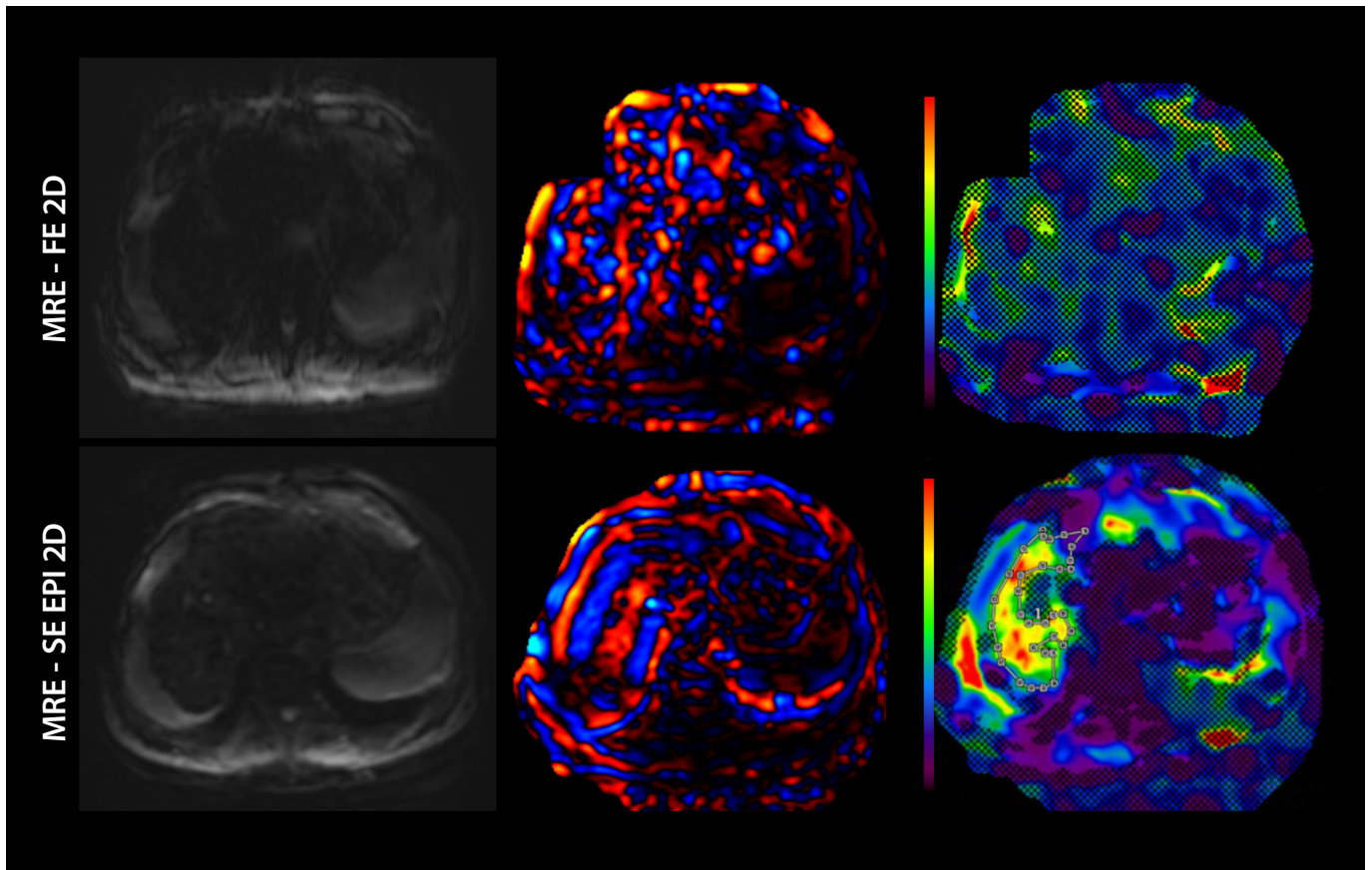


Figure 2: Top row: FE 2D MRE acquisition demonstrating the reduced SNR in the amplitude (left image) due to elevated $R2^*$ measurements (shortened $T2^*$), incoherent colored wave (middle image), and unreliable stiffness map (right image). Lower row: a successful MRE exam on the same patient using the SE-EPI 2D sequence, demonstrating a significant increase in liver stiffness measurements (Averaged 4.6 kPa).

Case 2

History: A 40-year-old male patient participated in the study for patients at risk for Metabolic dysfunction-associated steatotic liver disease (MASLD). The patient has no history of liver disease, and is not diabetic, but has a BMI of 35.0.

Imaging Findings: Clinical images were acquired on the Canon Galan 3T MRI and Canon Aplio i800 ultrasound system. Imaging findings demonstrated that the patient had severe steatosis with a median ATI of 0.91 dB/cm/MHZ (S3). Similarly, MR PDFF showed elevated liver fat measurements averaging

33.2%, and normal MR $R2^*$ measurements averaged 62.27/sec, as shown in Figure 3. MR PDFF and ultrasound ATI results are consistent with a finding of severe steatosis (S3).^{5,8}

MRE exams have demonstrated normal stiffness measurements using both FE 2D and SE-EPI 2D MRE sequences (2.5 kPa and 2.37 kPa, respectively) as shown in Figure 4. Similarly, the ultrasound SWE exam demonstrates normal measurements (shear wave speed median = 1.20 m/s) (Fig.4). Both MRE and ultrasound SWE measurements are within normal limits suggesting no or mild fibrosis. Therefore, the patient is unlikely to have Metabolic Dysfunction-Associated Steatohepatitis (MASH).^{6,9}

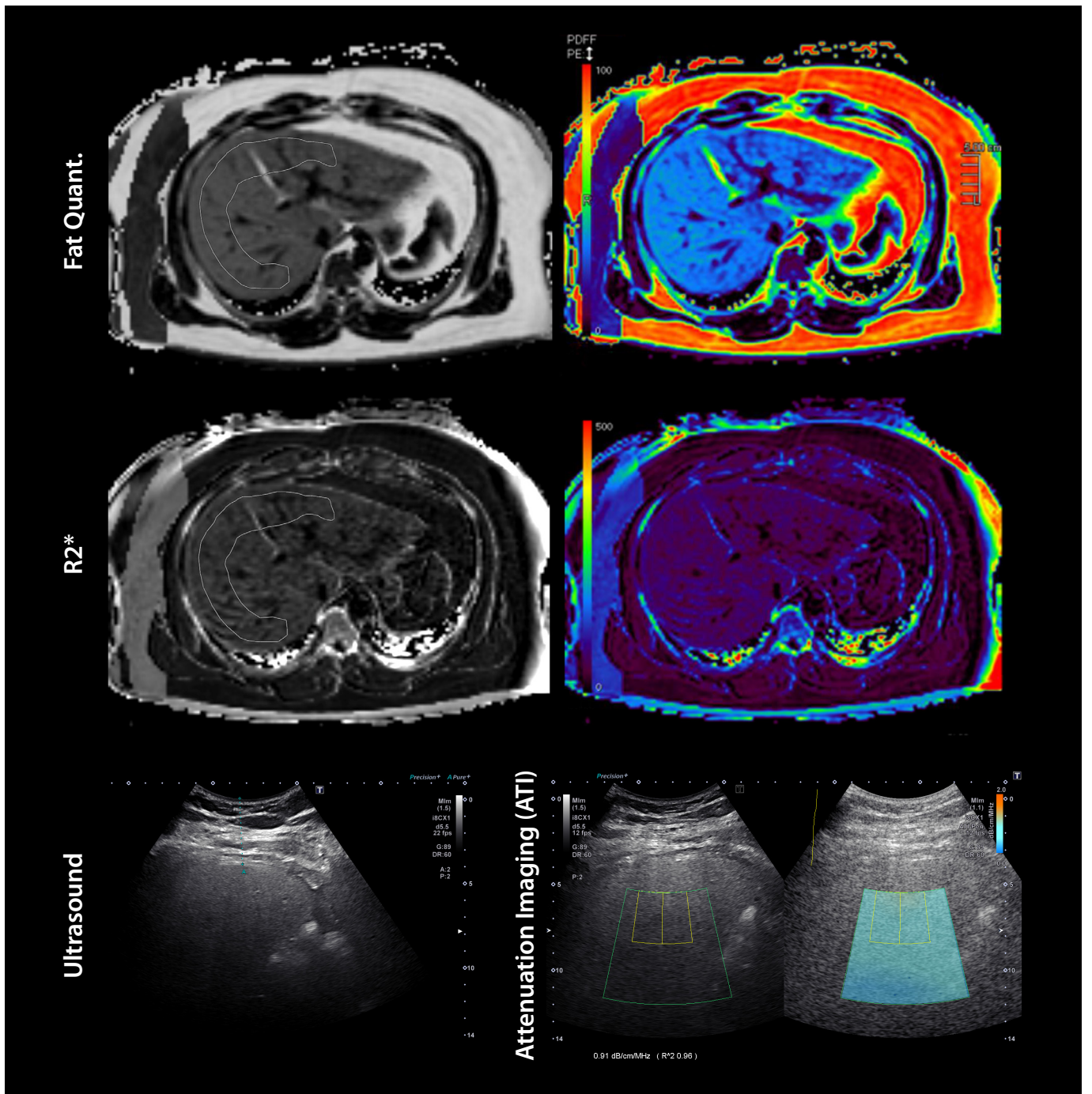


Figure 3: Top row: Fat quantification map from the axial mecho FE 3D PDFF scan with elevated fat measurements averaged 33.2% and colored map. Middle row: Generated transverse relaxation rate $R2^*$ and colored maps with normal $R2^*$ measurements (62.27/sec). Bottom row: Gray-scale ultrasound and median ATI (0.91 dB/cm/MHz) were consistent with a finding of severe steatosis (S3).

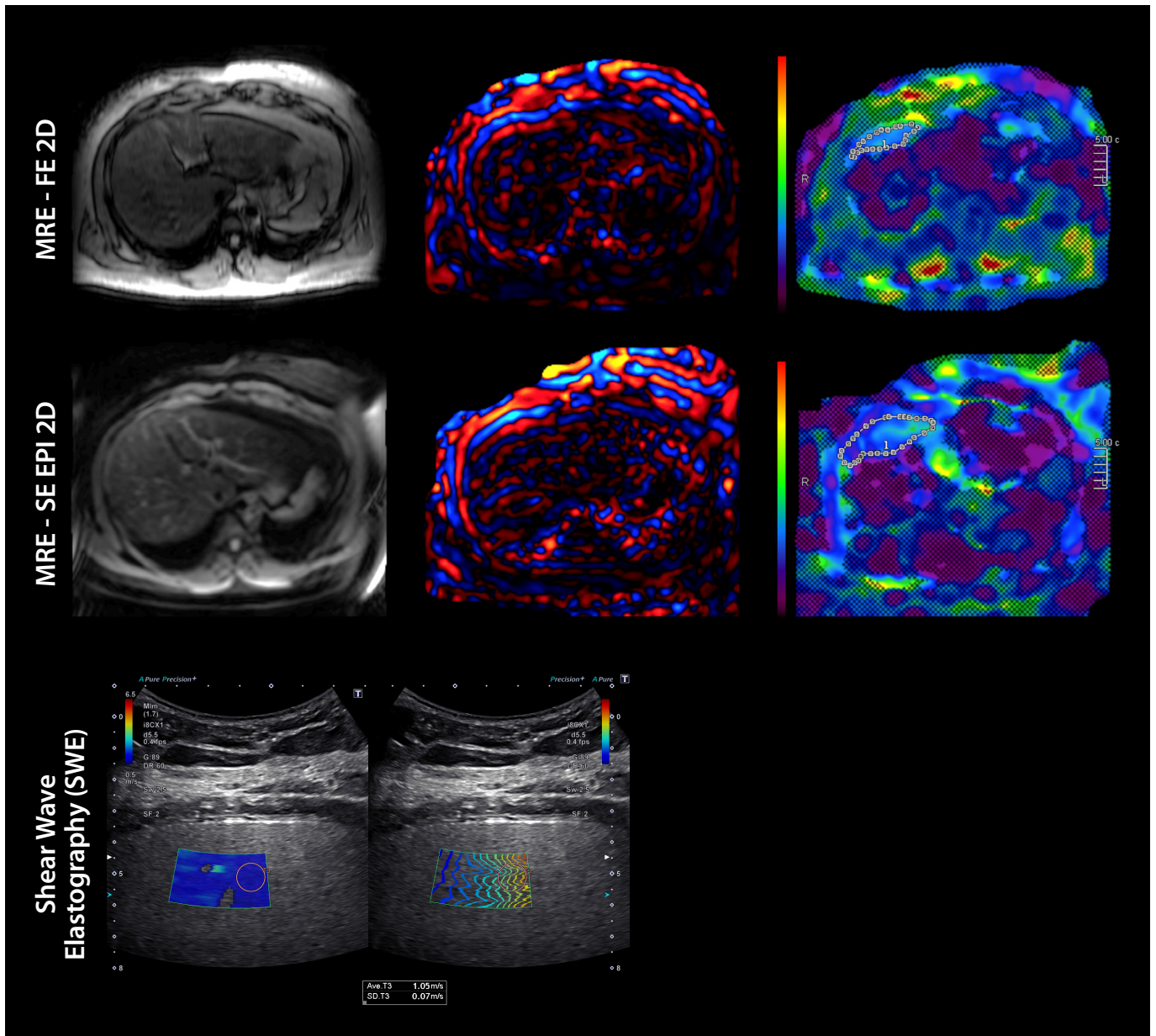


Figure 4: Example images of the two MRE acquisitions using FE 2D (top row) and SE EPI 2D (middle row) showing the magnitude images (left), colored wave images (middle), and colored stiffness maps (right). MRE exams have demonstrated normal stiffness measurements using both sequences (2.5 kPa and 2.37 kPa, respectively). Bottom row: Ultrasound shear wave elastography results also demonstrated normal liver stiffness (median shear wave speed 1.2 m/s).

Discussion

A comprehensive liver exam was performed on both patients. In case #1, the patient has a history of alcoholic liver cirrhosis. In addition to the clinical routine liver imaging techniques, advanced quantitative imaging biomarkers (e.g., PDFF, MRE, SWE, ATI) are critically important for managing such liver cases. In case #1, the increase in R2* measurements (shortened T2*), explains the unreliable MRE exam using the FE 2D sequence, as SNR of gradient-echo sequences are more susceptible to T2* changes. However, the availability of another base sequence for MRE using SE-EPI enabled a successful MRE exam to assess liver stiffness. In cases with unreliable ultrasound SWE (e.g., high IQR/median), MRE remains an effective method for determining liver stiffness non-invasively.³

In case #2, the patient had no history of liver disease. While

MRE, ultrasound SWE, and R2* measurements were normal, the PDFF and ATI exams demonstrated severe liver fat content. This plays a vital role in patient management and clinical outcomes. This patient is at risk for the development of MASH. Identifying MASLD at an early stage can lead to the reversal of the patient's steatotic liver disease and the prevention of progression to MASH.

Conclusion

With the increasing prevalence of CLD, quantitative imaging biomarkers of liver fibrosis, fat, and iron are emerging as critical tools for patient management. This case study demonstrates how Canon's multi-parametric tools for MRI and ultrasound enable confident and comprehensive liver exams.

Acknowledgments

The authors would like to thank Brian Tymkiw, Hung Do Ph.D., Dawn Berkeley, Karen Wager, and Mo Kadbi Ph.D. for their support when preparing this case study.

¹ R2* map is not FDA 510(k) cleared to calculate liver iron content.

The clinical results described in this case study are the experience of the author. Results may vary due to clinical setting, patient presentation, and other factors.

References

1. A. M. Moon, A. G. Singal, and E. B. Tapper, "Contemporary Epidemiology of Chronic Liver Disease and Cirrhosis," *Clin Gastroenterol Hepatol*, vol. 18, no. 12, pp. 2650–2666, Nov. 2020, doi: 10.1016/j.cgh.2019.07.060.
2. C. Estes, H. Razavi, R. Loomba, Z. Younossi, and A. J. Sanyal, "Modeling the epidemic of nonalcoholic fatty liver disease demonstrates an exponential increase in burden of disease," *Hepatology*, vol. 67, no. 1, pp. 123–133, Jan. 2018, doi: 10.1002/hep.29466.
3. G. Xiao, S. Zhu, X. Xiao, L. Yan, J. Yang, and G. Wu, "Comparison of laboratory tests, ultrasound, or magnetic resonance elastography to detect fibrosis in patients with nonalcoholic fatty liver disease: A meta-analysis," *Hepatology*, vol. 66, no. 5, pp. 1486–1501, Nov. 2017, doi: 10.1002/hep.29302.
4. R. Labranche *et al.*, "Liver Iron Quantification with MR Imaging: A Primer for Radiologists," *RadioGraphics*, vol. 38, no. 2, pp. 392–412, Mar. 2018, doi: 10.1148/rg.2018170079.
5. C. Hobeika *et al.*, "Ultrasound-based steatosis grading system using 2D-attenuation imaging: An individual patient data meta-analysis with external validation," *Hepatology*, p. 10.1097/HEP.0000000000000895, doi: 10.1097/HEP.0000000000000895.
6. G. Ferraioli *et al.*, "WFUMB Guideline/Guidance on Liver Multiparametric Ultrasound: Part 1. Update to 2018 Guidelines on Liver Ultrasound Elastography," *Ultrasound in Medicine & Biology*, vol. 50, no. 8, pp. 1071–1087, Aug. 2024, doi: 10.1016/j.ultrasmedbio.2024.03.013.
7. F. F. Guglielmo *et al.*, "Liver Fibrosis, Fat, and Iron Evaluation with MRI and Fibrosis and Fat Evaluation with US: A Practical Guide for Radiologists," *RadioGraphics*, vol. 43, no. 6, p. e220181, Jun. 2023, doi: 10.1148/rg.220181.
8. G. Ferraioli *et al.*, "WFUMB Guidelines/Guidance on Liver Multiparametric Ultrasound. Part 2: Guidance on Liver Fat Quantification," *Ultrasound in Medicine & Biology*, vol. 50, no. 8, pp. 1088–1098, Aug. 2024, doi: 10.1016/j.ultrasmedbio.2024.03.014.
9. R. G. Barr, S. R. Wilson, D. Rubens, G. Garcia-Tsao, and G. Ferraioli, "Update to the Society of Radiologists in Ultrasound Liver Elastography Consensus Statement," *Radiology*, vol. 296, no. 2, pp. 263–274, Aug. 2020, doi: 10.1148/radiol.2020192437.

Canon

CANON MEDICAL SYSTEMS USA, INC

<https://us.medical.canon>

2441 Michelle Drive, Tustin, CA 92780 | 800.421.1968

©Canon Medical Systems, USA 2024. All rights reserved. Design and specifications are subject to change without notice.

Made for Life is a trademark of Canon Medical Systems Corporation.

MRC514674US

Made For life